J. Phys. B: At. Mol. Opt. Phys. **29** (1996) L881–L888. Printed in the UK

LETTER TO THE EDITOR

Structure of the photodetachment cross section in a magnetic field: an experiment with OH^-

J D Rudmin†, L P Ratliff‡, J N Yukich§ and D J Larson†

† Department of Physics, University of Virginia, Charlottesville, VA 22903, USA
‡ Atomic Physics Division, NIST, Gaithersburg, MD 20899, USA
§ Department of Physics, University of Michigan, Ann Arbor, MI 48109, USA

Received 19 August 1996, in final form 25 October 1996

Abstract. Photodetachment from OH^- in a magnetic field has been studied experimentally using light with energies between 14 400 and 14 900 cm^{-1}. Presented here are high-resolution data which exhibit sharp magnetic field structure at thresholds and low-resolution data which show monotonically increasing cross sections. The current work is the first in any atomic or molecular system where sufficient energy resolution has been achieved to observe the shape of the cross section in a magnetic field.

Since the initial work of Blumberg *et al* [1, 2], photodetachment from negative ions in a magnetic field has been a topic of continuing interest [3–11]. The theoretical cross section rises sharply just above threshold and then decreases with energy. It differs greatly from the usual zero-field Wigner cross section [12, 13] which increases monotonically with energy. The current work was motivated in part by previous experimental work which clearly showed the non-monotonic character of the magnetic-field cross section [1, 4], but did not show its detailed shape. While the previous data, to the extent that they provided information about the shape, were consistent with the predicted shape of the cross section, experiments with O^-, S^- and Se^- showed significant discrepancies with theory in the relative magnitudes of the partial cross sections for different magnetic thresholds [1, 4, 7, 14].

We chose to study photodetachment from OH^- because it has a relatively simple spectrum; the energy levels of OH^- and OH have been measured with good precision [15, 16]; the few rotational states which are populated are well separated in energy and photodetachment from OH^- has been well studied in the absence of magnetic fields [15, 17]. It is interesting to note that OH has a relatively large dipole moment (0.65 ea_0) which interacts with the departing electron. Effects of this interaction have been seen in photodetachment from OH^- in the absence of magnetic fields [15, 18–22]. One might expect to find such effects in photodetachment in magnetic fields as well. The structure of the ground-state OH^- ion is simple because the orbital and spin angular momenta of the electron are both zero. The neutral OH molecule can be described by either the Hund's case a inverted or the Hund's case b angular momentum coupling schemes [23].

The cross section for photodetachment can be described by Fermi's golden rule: $\sigma_{if} \propto I_{if}\rho(E_f)$, where $I_{if} = |\langle f|\boldsymbol{E}\cdot\boldsymbol{r}|i\rangle|^2$. Near threshold, the electron detached from OH^- departs with zero angular momentum. Because the initial-state wavefunction has very short range relative to the wavelength of the departing electron, I_{if} is independent of energy to

0953-4075/96/240881+08$19.50

first order with momentum-normalized states, and the shape of the partial cross section near a given threshold depends only upon $\rho(E_f)$, the density of final states of the free electron. I_{if} gives the relative magnitude of the cross section at each threshold and depends on the projection of angular momentum states. When a magnetic field is absent, $\rho(E_f) \propto k$, the momentum of the detached electron. Near a particular threshold then, $\sigma_{if} \propto \sqrt{h\nu - E_{if}}$, which is the Wigner threshold law for detachment into an s-wave continuum. Here, $h\nu$ is the energy of the light illuminating the ion, and E_{if} is the energy required to detach the electron.

When a magnetic field is present, the states of a free electron lie on coaxial cylinders in momentum space. So the number of states which lie on a cylinder in momentum space $N_k \propto (2\pi k_c)k_z$, where k_c is the momentum radius of the cylinder and k_z is the momentum of the electron along the magnetic field. Then $\sigma_{if} \propto 1/\sqrt{k^2 - k_c^2} \propto 1/\sqrt{h\nu - E_{if}}$. This cross section, which rises discontinuously at each threshold and then falls, is resolvable for high magnetic fields. For low magnetic fields, individual partial cross sections are so closely spaced that only the monotonically increasing zero-field cross section is apparent.

The energy of a transition depends on the rotational and magnetic energies of initial and final states. To first order, the rotational energy is $E_{rot} = B(J - \Lambda - S)^2$, where J and S are the total and spin angular momentum quantum numbers and $B = 18.7409(45)$ cm^{-1} for OH^- and $B = 18.5310$ cm^{-1} for OH is the rotational constant [15, 16]. $\Lambda = L_z$ is the projection of the orbital angular momentum along the internuclear axis. The magnetic threshold energies are

$$E(J', M', m_e, n, M'') = E(J', M') + \mu_0 H(g_e m_e + 2(n + \tfrac{1}{2}) - g'' M'') + \mathrm{EA} \tag{1}$$

where the g's are the gyromagnetic ratios, n is the electron cyclotron quantum number and EA $= 14\,703.6(1)$ cm^{-1} is the electron affinity [15]. Double primes refer to the negative ion and single primes refer to the neutral atom. The electron's gyromagnetic ratio is $g_e \approx 2$, and the gyromagnetic ratio of OH^- is $g'' \approx 0$ because $L'' = S'' = 0$. $E(J', M')$ is calculated using Hill's method [24] for a state intermediate between Hund's cases a and b, where we find the projection along the magnetic field $\boldsymbol{H}$ of the average orbital angular momentum $\boldsymbol{L}$ and spin $\boldsymbol{S}$:

$$\begin{aligned} E(J', M') &= \mu_0 \boldsymbol{H} \cdot (\bar{\boldsymbol{L}} + 2\bar{\boldsymbol{S}})/\boldsymbol{J}^2 = \mu_0 H M_J (\Omega\Lambda + 2\boldsymbol{J} \cdot \bar{\boldsymbol{S}}) \\ &= B[f(J', M') \pm \tau(J', M')/2] \end{aligned} \tag{2}$$

where

$$\begin{aligned} f(J', M') &= \left(J' + \tfrac{1}{2}\right)^2 - \Lambda^2 + \beta\left(\Lambda^2 + \tfrac{1}{2}\right) \\ \tau(J', M') &= \sqrt{(2J' + 1)^2(1 - \beta)^2 + \Lambda^2(Y + \beta)(Y - 4 + 5\beta)} \\ \beta &= (4.67 \times 10^{-5}\ H\ \mathrm{cm}^{-1}\ M')/(B J'(J' + 1)) \end{aligned}$$

and $\Omega = J_z$ is the projection of the total angular momentum along the internuclear axis, and Y is the ratio of the spin–orbit coupling constant $A = -139.7$ cm^{-1} [17] to the rotational constant B [23]. A is negative because the $^2\Pi_{3/2}$ state is lower in energy than the $^2\Pi_{1/2}$ state.

The molecular dipole moment of OH is not observable while the molecule is in a state of definite parity. However, the departing electron may mix Λ-doubled states, inducing a dipole moment. To conserve parity of the system, the electron detaches into a state of mixed parity, which, in the absence of a magnetic field, should result in a cross section which rises slowly very near threshold and then rises rapidly [19]. For the transition presented here, to $^2\Pi_{3/2}$ $J' = \frac{3}{2}$, the Λ-doubled states are split by only 0.055 cm^{-1} [25]. This is less than the resolution of the experiment and much less than the cyclotron energy of 1.2 cm^{-1}. Under

these conditions, one might see dipole interaction effects such as a shift in the first threshold [10, 11], a modification of the energy dependence of the cross section [21, 26], or a small change in the spacing of cyclotron levels [10, 27].

To calculate the relative strength of a transition, we consider the transition of the angular momentum of the negative ion (J'', M'') to that of an intermediate basis (J_i, M_i), to that of the final neutral atom (J', M') plus the free electron [23, 28]:

$$I_{if} = I(J'', M'', J', M', m_e) \propto \left| \sum_{J_i=J'\pm 1/2} \sum_{M_i=-J_i}^{J_i} \sum_{\Omega=1/2}^{3/2} \left\langle u_\alpha J' | {}^2\Pi_\Omega, J', M'; ks, \tfrac{1}{2}, m_e \right\rangle \times \left\langle {}^2\Pi_\Omega, J', M'; ks, \tfrac{1}{2}, m_e | {}^1\Pi, J_i, M_i \right\rangle \left\langle {}^1\Pi, J_i, M_i | r | {}^1\Sigma, J'', M'' \right\rangle \right|^2 . \tag{3}$$

From right to left, the projections represent: absorption of a photon, projection to a basis with a free electron of momentum k, spin s and a neutral molecule in a Hund's case a inverted basis, and projection of the case a states onto the molecular states which are intermediate between Hund's case a inverted and Hund's case b. To calculate the leftmost projection, we calculate the rotational energy in the Hund's case a basis with parity symmetry and add the spin–orbit perturbation. We then diagonalize the resulting matrix to obtain the energies in (2), and the molecular states:

$$|u_\alpha J'\rangle = c_1 \left| {}^2\Pi_{1/2}, J'; ks, \tfrac{1}{2} \right\rangle + c_2 \left| {}^2\Pi_{3/2}, J'; ks, \tfrac{1}{2} \right\rangle \tag{4}$$

where

$$c_1 = \sqrt{\frac{\tau - 2 + Y}{2\tau}} \qquad \text{and} \qquad c_2 = -\sqrt{\frac{\tau + 2 - Y}{2\tau}} \, . \tag{5}$$

We evaluate the other projections using finite rotation matrices [29], and we obtain

$$I(J'', M'', J', M', m_e) \propto \left| \sum_{J_i} (2J_i + 1) \sqrt{(2J' + 1)(2J'' + 1)} \times \begin{pmatrix} J' & \frac{1}{2} & J_i \\ M' & m & -M_i \end{pmatrix} \begin{pmatrix} J_i & 1 & J'' \\ M_i & -p & -M'' \end{pmatrix} \begin{pmatrix} J_i & 1 & J'' \\ 1 & -1 & 0 \end{pmatrix} \times \left[c_1 \begin{pmatrix} J' & \frac{1}{2} & J_i \\ \frac{1}{2} & \frac{1}{2} & -1 \end{pmatrix} + c_2 \begin{pmatrix} J' & \frac{1}{2} & J_i \\ \frac{3}{2} & -\frac{1}{2} & -1 \end{pmatrix} \right] \right|^2 . \tag{6}$$

This function describes a high-resolution cross section where individual magnetic transitions are resolved. If we wish to retrieve the form in Schultz *et al* which is independent of magnetic quantum numbers, and which is appropriate for low-resolution data, then we sum over m, M' and M'' outside the absolute square [23]†.

In the experiment, OH^- ions were created in a Penning ion trap [1, 30] by dissociative attachment of thermal electrons to water vapour at 10^{-8} Torr. The trap confined the ions to a region roughly 1 mm in radius with a magnetic field of 1.2 T and a potential difference of -1.4 V between the endcap and ring electrodes.

Single-mode light was produced by a ring dye laser pumped by an argon ion laser. The wavelength was measured by a travelling interferometer wavelength meter using a polarization-stabilized HeNe laser as a reference. Excitation in an iodine vapour cell provided absolute wavelength calibration. The light was directed into the trap with propagation direction perpendicular to the magnetic field and linear polarization along the

† There is an omission in (11) of [23] for the transition $J' = J'' + \frac{3}{2}$. The denominator should read $2(J'' + 3)$ instead of $2J'' + 3$.

field. To ensure that the ions were illuminated with the same photon flux in each data cycle, a photodiode was used to measure the amount of light passing through the trap. A shutter blocked the light when the total integrated power reached a preset value. Although one-photon detachment depends linearly on laser power, collisional redistribution of ion rotational states makes detachment a function of illumination time. To keep illumination times constant, the light intensity was stabilized by a commercial 'noise eater'.

The data are the fractions of ions surviving illumination as a function of the wavelength of the light. Two different kinds of data were taken. Low-resolution data were taken with 7 cm^{-1} point spacing, with laser powers ranging from 25 to 75 mW and interaction times ranging from 0.4 to 1.5 s. The function used to fit the low-resolution data, f_{LoRes}, has a value of *one* for frequencies below the lowest threshold and falls toward *zero* above each threshold, as the total cross section increases:

$$f_{\mathrm{LoRes}} = A \sum_{J''} (2J'' + 1) \mathrm{e}^{E''/k_{\mathrm{B}}T} \mathrm{e}^{-\Phi t \sum_{J'} \sigma_{J''J'}}. \tag{7}$$

Here A is the normalization, E'' is the rotational energy of the initial state of the ion, T is the rotational temperature of the ions, Φt is the photon flux and $\sigma_{J''J'}$ is the cross section

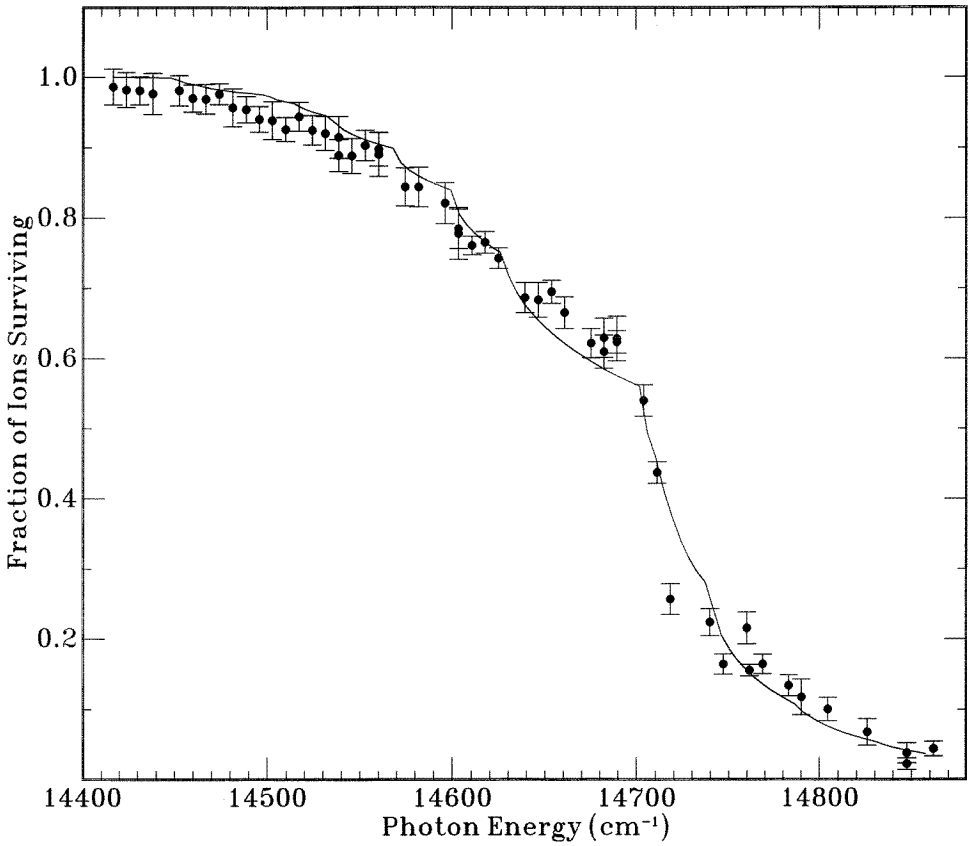

Figure 1. Low-resolution scan of the OH^- photodetachment spectrum. The number of ions surviving illumination decreases as the cross section increases. These data cover many rotational thresholds. The sharp feature near 14 703 cm^{-1} is the threshold for detachment from $J'' = 1$ to $J' = \frac{3}{2}$, $\Omega = \frac{3}{2}$.

for detachment from the initial state with angular momentum from J'' to the final state with angular momentum J'. Because individual magnetic transitions are not resolved here, we use the Wigner law cross section [13] with the relative weightings for different thresholds given by (6) summed over the magnetic quantum numbers.

To account for Doppler broadening and other sources of broadening, f_{LoRes} is convolved with a Gaussian function. This model is used to fit the data to obtain a rotational temperature and integrated laser power. The data show good agreement with the model, except that they tend to show slightly more detachment than the model for low photon energy (see figure 1). The rotational temperature of the ions determines the relative amplitudes of the rotational thresholds. This temperature, 280(20) K, is the lowest that has been seen in our apparatus. Previous measurements on SH^- and SeH^- showed temperatures of 745(36) K and 1100(50) K, respectively [27, 31]. The relatively low rotational temperature in OH^- is likely to be coupled to a similar translational temperature due to evaporation from the relatively small trapping potential used in these experiments. The ion temperature seems to be proportional to the trapping potential, as is expected.

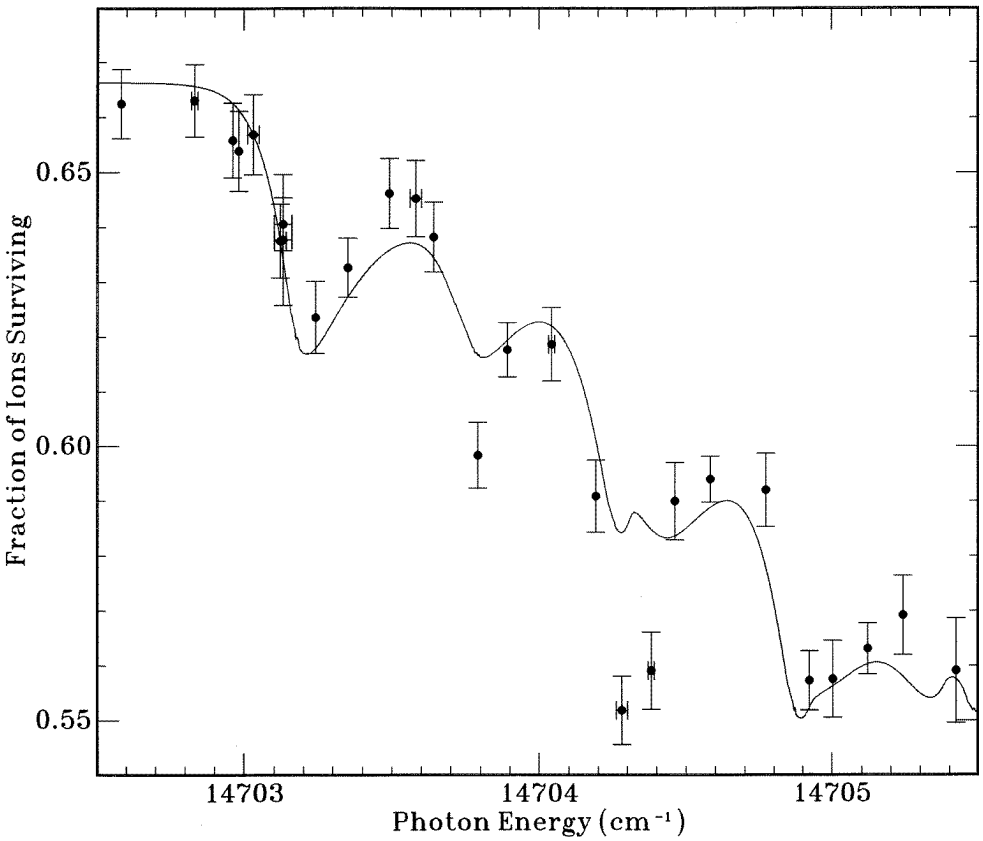

Figure 2. High-resolution scan of the threshold for detachment from $J'' = 1$ to $J' = \frac{3}{2}$, $\Omega = \frac{3}{2}$. Multiple thresholds result from magnetic-field splitting of a single rotational threshold. The data exhibit the sharp peaked structure predicted for the cross section for photodetachment in a magnetic field of 1.2 T. $\chi^2_{\mathrm{R}} = 2.78$; $E_0 = 14\,703.379(16)$ cm^{-1}; fixed $T = 280$ K.

In addition to the broad, low-resolution scans, we took very narrow, higher resolution scans with relatively high intensity (80 mW) light and point spacing on the order of 0.1 cm^{-1}. In the high-resolution scans the magnetic structure becomes resolvable. The function used to fit these data was

$$f_{\mathrm{HiRes}} = A \sum_{M''=-J''}^{J''} \mathrm{e}^{-\Phi t \sum_{M'=-J'}^{J'} \sigma_{M'M''}} \tag{8}$$

where A is the fraction of initial ions with total angular momentum J'', $\sigma_{M'M''}$ is the cross section for detachment from an initial state with angular momentum $J''M''$ to a final state with angular momentum $J'M'$. Here we use the cross section in a magnetic field, k^{-1} [2, 8], with motional Stark broadening and Doppler broadening added [2] and with the relative weightings for different thresholds given by (6). At the relatively low temperatures in these experiments, the major effects of the broadening are to reduce the slope of the cross section near threshold and to limit the height of the peak in the cross section, thus increasing the apparent width. Motional broadening is the only significant broadening in the experiment; the motional broadening is approximately 0.2 cm^{-1}, and is much larger than the laser linewidth which is less than 3×10^{-5} cm^{-1}. We usually fit to four or five

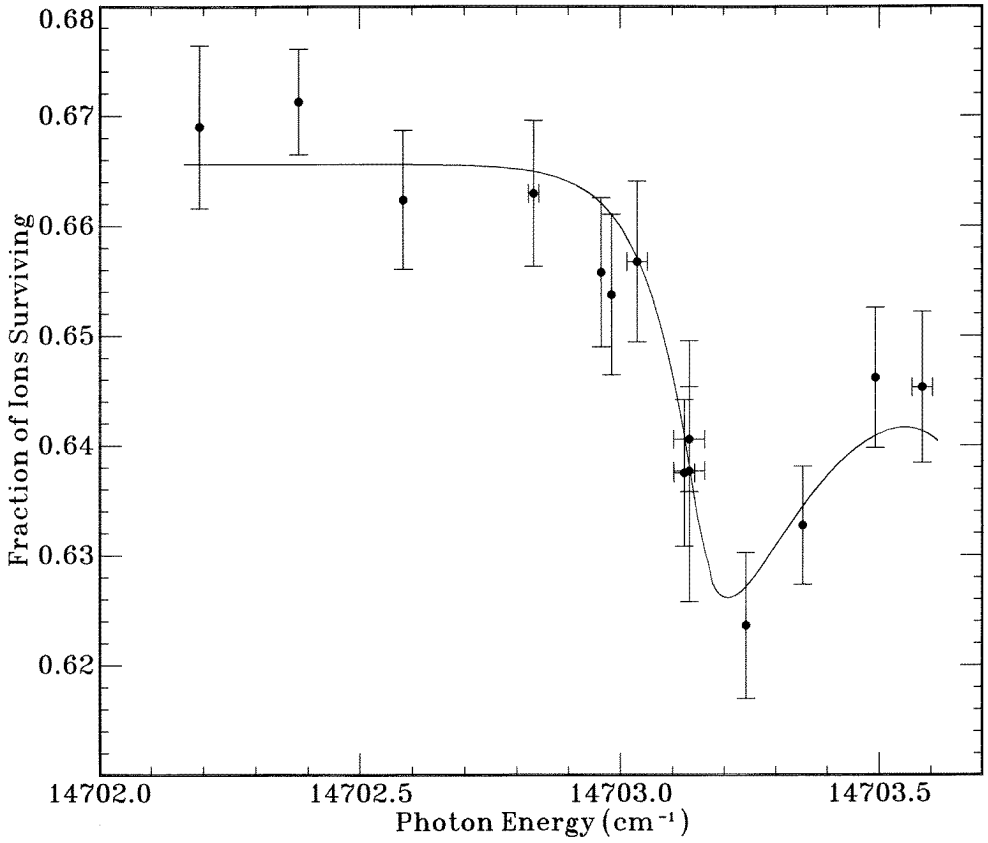

Figure 3. High-resolution frequency scan and theoretical fit to the first magnetic threshold of the transition from $J'' = 1$ to $J' = \frac{3}{2}$, $\Omega = \frac{3}{2}$. ($M'' = 1$ to $M' = -\frac{1}{2}$, $m_e = -\frac{1}{2}$, $\Lambda = 1$, $n = 0$.) $\chi^2_R = 0.574$; $E_0 = 14\,703.369(15)$ cm^{-1}; $T = 300(100)$ K.

parameters: A, the electron affinity, the translational temperature of the ions, the photon flux, Φt, and the intensity of the magnetic field. This description of the cross section at high resolution is the same as that at low resolution, except that the rotational temperature is accounted for in A, since only one rotational threshold is described. There are $(2J'' + 1)$ magnetic thresholds for each rotational threshold.

The best resolution was available near the threshold for the transition from $J'' = 1$ to $J' = \frac{3}{2}$, $\Omega = \frac{3}{2}$, near 14 703 cm^{-1}. This transition has a large partial cross section and there is a large population in the $J'' = 1$ state at 280 K. Two different fits to the data are shown in figures 2 and 3, and the caption for each gives the fit's reduced chi-squared, χ^2_R, zero-field threshold, E_0, and the temperature, T. The data in figure 2 are fitted to the fixed temperature of 280 K obtained for the rotational state distribution from the fit shown in figure 1. We fix the temperature because when temperature is a free parameter, fits to the intensities of the second and third features result in unrealistically low temperatures of less than 100 K. From the data, the intensities of the second and third features appear to be about twice their theoretical values. Figure 3 shows a particularly good fit to the first magnetic threshold, which gives a translational temperature of 300 (100) K. We obtain consistent values for the zero-field threshold from all the fits, suggesting that accurate intensities are not absolutely necessary to obtain information about threshold energies. The zero-field threshold energy of 14 703.379(16) cm^{-1}, extracted from the fit of the four resolved magnetic thresholds of the rotational transition from $J'' = 1$ to $J' = \frac{3}{2}$, $\Omega = \frac{3}{2}$ disagrees with 14 703.6(1) cm^{-1} from Schulz *et al* [15]. The sharp asymmetric structure predicted for the magnetic field cross section is exhibited for the first time in these data. The discrepancy with the expected cross section is largely in the intensities of the partial cross sections, and possibly in the spacing of the magnetic thresholds.

Photodetachment from OH^- in a magnetic field has been observed at both high and low energy resolution. The experimental results fit reasonably well to theoretically predicted shapes and absolute energy levels. The low-resolution data give a map of rotational transitions. The high-resolution data give Landau level spacings, and give partial cross section strengths, and they exhibit the unique shape of the magnetic-field cross section. Future experiments will use higher magnetic fields to enhance the resolution and better quantify the energies of individual thresholds. We are also trying to understand better the effect of the molecular dipole moment on the shape of the cross section.

This work is supported in part by the US National Science Foundation.

References

[1] Blumberg W A M, Jopson R M and Larson D J 1978 *Phys. Rev. Lett.* **40** 1320
[2] Blumberg W A M, Itano W M and Larson D J 1979 *Phys. Rev.* A **19** 139
[3] Fabrikant I I 1991 *Phys. Rev.* A **43** 258
[4] Krause H F 1990 *Phys. Rev. Lett.* **64** 1725
[5] Du M L 1989 *Phys. Rev.* A **40** 1330
[6] Crawford O H 1988 *Phys. Rev.* A **37** 2432
[7] Elmquist R E, Fletcher C J and Larson D J 1987 *Phys. Rev. Lett.* **58** 333
[8] Greene C H 1987 *Phys. Rev.* A **36** 4236
[9] Stoneman R C and Larson D J 1987 *Phys. Rev.* A **35** 2928
[10] Stoneman R C and Larson D J 1986 *J. Phys. B: At. Mol. Phys.* **19** L405
[11] Clark C W 1983 *Phys. Rev.* A **83** 28
[12] Lineberger W C, Hotop H and Patterson T A 1976 *Electron and Photon Interactions with Atoms* ed H Kleinpoppen and M R C McDowell (New York: Plenum) p 125
[13] Wigner E P 1948 *Phys. Rev.* **73** 1002

[14] Edge C J 1988 *Doctoral Dissertation* University of Virginia, Charlottesville, VA
[15] Schultz P A, Mead R D, Jones P L and Lineberger W C 1982 *J. Chem. Phys.* **77** 1153
[16] Coxon J A 1980 *Can. J. Phys.* **58** 933
[17] Breyer F, Frey P and Hotop H 1981 *Z. Phys.* A **300** 7
[18] Mead R D, Stevens A E and Lineberger W C 1984 *Gas Phase Ion Chemistry* ed M T Bowers (Orlando, FL: Academic) p 213
[19] Engelking P C and Herrick D R 1984 *Phys. Rev.* A **29** 2425
[20] Herrick D R and Engelking P C 1984 *Phys. Rev.* A **29** 2421
[21] Engelking P C 1982 *Phys. Rev.* A **26** 740
[22] Hotop H, Patterson T A and Lineberger W C 1974 *J. Chem. Phys.* **60** 1806
[23] Schultz P A, Mead R D and Lineberger W C 1983 *Phys. Rev.* A **27** 2229
[24] Hill E L 1929 *Phys. Rev.* **34** 1507
[25] Meerts W L 1977 *Chem. Phys. Lett.* **46** 24
[26] Kobayashi T, Hinchcliffe R D and Engelking P C 1993 Private communication
[27] Mansour N B 1987 *Doctoral Dissertation* University of Virginia, Charlottesville, VA
[28] Rau A R P and Fano U 1971 *Phys. Rev.* A **4** 1751
[29] Zare R N 1988 *Angular Momentum, Understanding Spatial Aspects in Chemistry and Physics* (New York: Wiley)
[30] Dehmelt H 1967, 1969 *Advances in Atomic and Molecular Physics* vol 3, 5 ed D R Bates and I Estermann (New York: Academic)
[31] Stoneman R C 1985 *Doctoral Dissertation* University of Virginia, Charlottesville, VA